HEFAT2012
9th International Conference on Heat Transfer, Fluid Mechanics and Thermodynamics
16 – 18 July 2012
Malta

Comparison of Breakup Models for Large Space in High Pressure Pulse Sprays

R. Sagawa, Y. Kojima, Y. Saito and H. Aoki*
*Corresponding author
Department of Chemical Engineering,
Graduate School of Engineering, Tohoku University,
6-6-07 Aoba, Aramaki, Aoba-ku, Sendai 980-8579, Japan
E-mail: aoki@tranpo.che.tohoku.ac.jp

ABSTRACT

Optimization of breakup models for high-pressure pulse sprays in a stationary combustor was investigated by an experimental and numerical study. In the spray experiment, we measured the droplet distribution and spray flux under atmospheric pressure. We also conducted a numerical simulation of spray flow using various breakup models and compared the results with those obtained from our experiments to assess the numerical accuracy of the breakup models and propose a suitable breakup model for large spaces. The breakup of the droplets was calculated using three breakup models. The first two are widely used models—Taylor Analogy Breakup (TAB) model (O'Rourke and Amsden, 1987) and the modified KH–RT model. Besides, we propose a third breakup model that combines the KH and TAB models. The results of the proposed model, the KH–TAB model, are in good agreement with those obtained from our measurements. Hence, we conclude that the KH–TAB model is an appropriate breakup model for large spaces such as in the stationary combustor.

INTRODUCTION

Stationary combustors such as gas turbines or boilers are widely used in industry. The most commonly used combustion system is spray combustion. Combustors are undergoing development and optimization in order to comply with strict environmental regulations imposed on stationary combustors. Stationary combustors are designed with a common rail-injection system, which is used in internal-combustion engines for environmentally friendly combustion. Using this system, a high pressure fuel injection and injection timing and form pulse sprays are controlled. In a previous study [1], an internal-combustor-injection system was studied, focusing on a single spray in a small space. Because the stationary combustor space is large scale and the pulse sprays affect each other, it is necessary to evaluate the spray characteristics in free space.

Numerical simulations of fuel–air mixing for combustion have been investigated and breakup models representing spray combustion have been proposed [1-2]. Those breakup models focus on

internal-combustion engines and refer only to the droplet diameter and the spray shape around the nozzle tip [3-4]. While most breakup models are designed for a small space, hardly any breakup models have been reported for large spaces.

In this study, we carried out experimental and numerical investigations aimed at deriving an optimized breakup model for high-pressure pulse sprays in a stationary combustor. In the spray experiment, we first measured droplet distribution and spray flux under atmospheric pressure. We then conducted a numerical simulation of spray flow using various breakup models. The results of the numerical simulations were compared with those obtained from the experiments to assess the numerical accuracy of the breakup models, and a suitable breakup model for large spaces was proposed.

NOMENCLATURE

A	area	[m^2]
A, B	parameters in Nukiyama–Tanazawa distribution function	
B_0, B_1	constants in the KH model	
C_{RT}, C_τ	constants in the RT model	
C_μ, $C_{\varepsilon 1}$, $C_{\varepsilon 2}$	constants in the k–ε model	[-]
D	width	[m]
d_{32}	Sauter mean diameter	[m]
d_{max}	maximum particle diameter	[m]
f_N	particle number distribution function	[-]
f_V	volume distribution function	[-]
g	gravitational acceleration	[$m \cdot s^{-2}$]
G_k	production rate of kinetic energy	[$kg \cdot m^{-1} \cdot^{-3}$]
K	constants in the TAB model	
k	kinetic energy of turbulence	[$m^2 \cdot s^{-2}$]
L	breakup length	[m]
L_e	length scale of turbulent eddy	[m]
n	total number of particle	
p	Pressure	[Pa]
Re	Reynolds number	[-]
S_ϕ	source term for ϕ	
$S_{p,\phi}$	source term evaluated by the PSI-CELL model	
T	Taylor Number	[-]
t	time	[s]
u, v	velocity component	[$m \cdot s^{-1}$]
We	Weber number	[-]
r	droplets diameter	[m]
x, r	cylindrical coordinate	
y	drop distortion parameter	[-]
Z	Ohnesorge number	[-]

<Greek symbols>

α,β	parameters in Nukiyama–Tanazawa distribution function	
β_0	constants in the k–ε model	
ϕ	dependent variable	
Γ_ϕ	diffusion term for ϕ	[$kg \cdot m^{-1} \cdot s^{-1}$]
η_0	constants in k-ε model	
Λ	wavelength of the fast growing wave	[m]
μ	fluid viscosity	[Pa·s]
ρ	fluid density	[$kg \cdot m^{-3}$]
σ	surface tension	[$N \cdot m^{-1}$]
τ	breakup time	[s]
Ω	frequency of the fast growing wave	[s^{-1}]

<Subscripts>

f	Fluid
KH	Kelvin–Helmholtz
p	Particle
RT	Rayleigh–Taylor

Experimental

Experimental apparatus and conditions

A schematic diagram of the experimental apparatus is shown in Figure 1. Fuel passes the high-pressure common rail and is injected into the free space at room temperature and pressure. The spray is controlled by the injection controller (Figure 1). The nozzle diameter is 0.2 mm with a single hole (Figure 2). The experimental conditions are listed in Table 1. The oscillation frequency means frequency of injection in a second. For example, in the case of the oscillation frequency at 200 Hz, the spray is injected 200 times per second as shown in Figure 3. The fuel flow rate is constant.

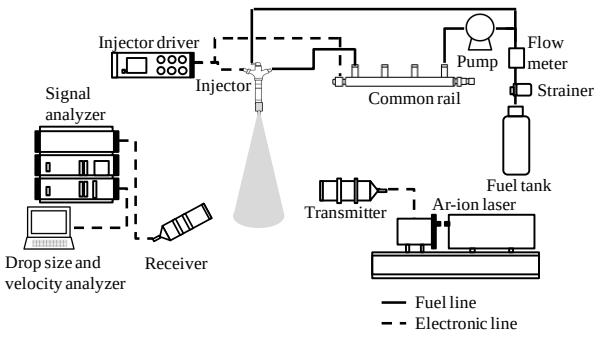

Figure 1 Schematic diagram of the experimental apparatus

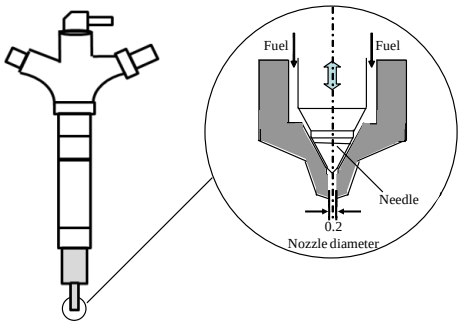

Figure 2 Schematic diagram of the high-pressure diesel fuel injector

Table 1 Experimental conditions

Fuel		Diesel
Fuel flow rate	[L/min]	0.1
Injection pressure	[MPa]	40
Nozzle diameter	[mm]	0.2
Oscillation frequency	[Hz]	200
Injection time	[ms]	1.34

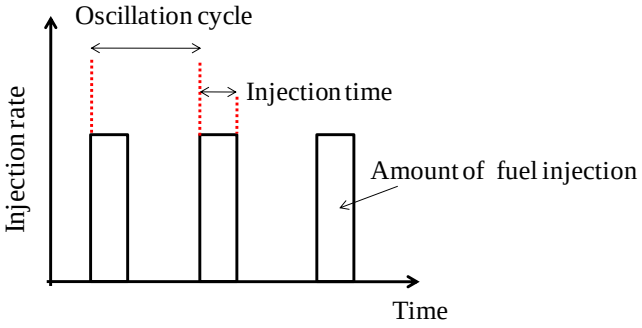

Figure 3 Image of the oscillation cycle and the injection time

Measurement of size distribution and spray flux

We carried out spray experiments under atmospheric pressure, and measured the droplet size distribution and spray flux. The measurements were made 200 mm downstream from the nozzle tip as shown in Figure 4.

The size distribution was measured by a phase Doppler particle analyzer (PDPA). When over 5,000 droplets were captured, the size distribution was evaluated by the Sauter mean diameter (SMD).

The spray flux was measured by the isokinetic suction probe system proposed by Yoshida[5]. Figure 5 shows a schematic diagram of the isokinetic suction probe system. Droplets were collected by isokinetic sampling and the spray flux was measured for 30 s at each measurement point. In this study, the droplet collection efficiency was above 90 %.

The resulting of spray characteristics were compared with those observed from numerical results.

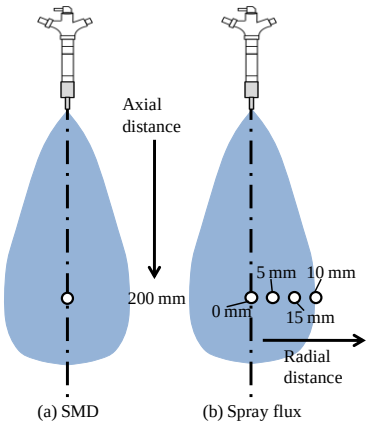

Figure 4 Measuring points of SMD and spray flux

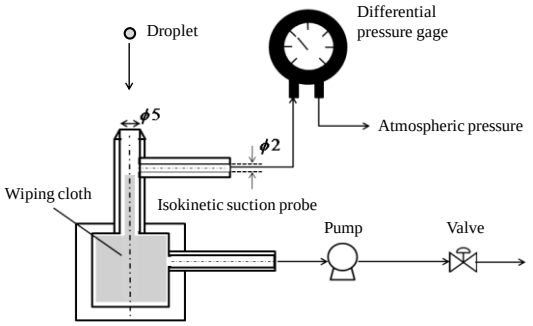

Figure 5 Schematic diagram of isokinetic suction probe system

Numerical simulation of spray flow

Analytical Object

The analytical object(Figure 6) is a two-dimensional spray flow. The computational domain is 300 mm × 150 mm in the x- and r-directions, respectively. The computational domain is divided into uniform 80×62 grids. We used non-uniform grids to reduce computational loads.

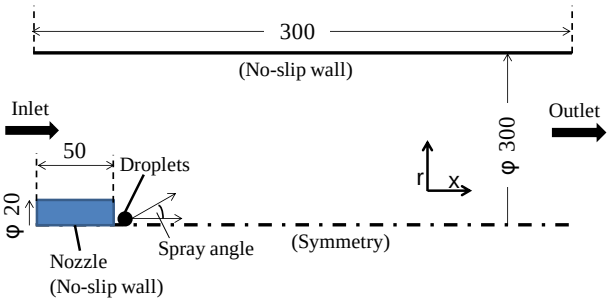

Figure 6 Analytical object

Governing equation and numerical schemes

The gas-phase flow field is described using the Navier–Stokes equations with the RNG k–ε turbulence model. The governing equations for the fluid flow system are

$$\frac{\partial \rho\phi}{\partial t}+\frac{\partial}{\partial x}(\rho U\phi)+\frac{1}{r}\frac{\partial}{\partial r}(r\rho V\phi)= \frac{\partial}{\partial x}\left(\Gamma_\phi\frac{\partial \phi}{\partial x}\right)+\frac{1}{r}\frac{\partial}{\partial r}\left(r\Gamma_\phi\frac{\partial \phi}{\partial r}\right)+S_\phi+S_{p\phi}\ , \quad (1)$$
$$\phi = 1(mass), u, v, k, \varepsilon\ ,$$

where $S_{p\phi}$ is an additional source term from the particle phase, and is evaluated by the PSI-CELL model [6]. These equations are discretized using the finite volume method (FVM). The simplified marker and cell (SMAC) method is applied as the coupling scheme. The numerical schemes are summarized in Table 3.

In the spray phase, the motion of the droplets in the turbulent flow field is calculated by the Lagrangian method.

Table 3 Numerical schemes

Discretization method	Finite volume method
Discretization scheme for momentum equation	
Convection term	SUPERBEE [7]
Diffusion term	2nd-order central difference
Discretization scheme for the k–ε equation	
Convection & diffusion	Hybrid difference
Unsteady term	1st-order Euler explicit
Coupling scheme	SMAC
Matrix solver	AMGS (for p)
	SOR(for k–ε)

Numerical conditions

Table 4 shows numerical conditions. The injection time and spray cone angle were obtained from the experimental results. Air and diesel properties are used for the gas and droplet parameters (Table 5).

Table 4 Numerical conditions

Injection pressure	[MPa]	40
Injection time	[ms]	1.34
Initial droplets diameter	[mm]	0.21
Spray angle	[deg]	7
Initial air velocity	[m・s^{-1}]	0.1
Initial droplets velocity	[m・s^{-1}]	198

Table 5 Air and droplet properties

Density, ρ_g	[kg・m^{-3}]	1.184
Viscosity, μ_g	[Pa・s]	1.84×10^{-5}
Density, ρ_p	[kg・m^{-3}]	850
Viscosity, μ_p	[Pa・s]	2.62×10^{-3}
surface tension, σ_p	[mN・m^{-1}]	26.3

The breakup model

The breakup of the droplets was calculated using three breakup models. The first two breakup models—the TAB model by O'Rourke and Amsden[8] and the modified KH–RT model—are widely used. Here we propose a third breakup model that combines the KH and TAB models.

The droplet analysis of droplets is based on the Lagrangian method. When a droplet breaks up, the initial droplets diameter is equal to the nozzle diameter.

The TAB model

The original TAB model describes the droplet deformation and breakup in sprays. The model is based on an analogy between an oscillating droplets exposed to an air flow field and a forced oscillating spring-mass system, as seen in Figure 7. Using the dimensionless displacement of the droplet y (=2x/r), the equation of droplet motion is

$$\ddot{y} + \frac{5\mu_p}{\rho_p r^2}\dot{y} + \frac{8\sigma}{\rho_p r^3} y - \frac{2}{3}\frac{\rho_f u_r^2}{\rho_p r^2} = 0. \quad (2)$$

After solving this ordinary differential equation, y is given by the following.

$$y(t) = \frac{We}{12}(1 - \cos pt) \quad (3)$$

$$\frac{dy}{dt} = \frac{We}{12} p \sin pt \quad (4)$$

$$We = \frac{\rho_f u_r^2 r}{\sigma}, \quad p = \sqrt{\frac{8\sigma}{\rho_p r^3}} \quad (5)$$

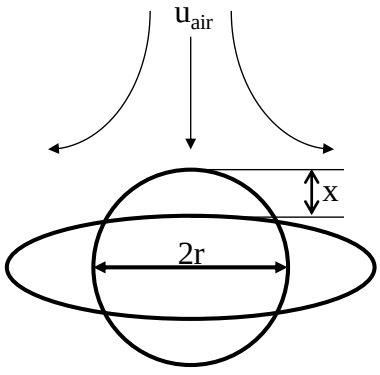

Figure 7 The TAB model[8]

The equation of the droplet size after breakup is based on the analysis of energy conservation between the parent droplet and the product droplet. The mean size of the product droplets r_{32} is derived as

$$r_{32} = \frac{r}{1 + \frac{8K}{20} + \frac{6K}{120}\frac{5}{\sigma}\frac{\rho_p r^3}{\sigma}\dot{y}^2}, \quad (6)$$

where the model constant K is 10/3. After the breakup, the product droplet size is chosen randomly from the Nukiyama–Tanasawa distribution, and the number of product droplets can be predicted using the law of mass conservation. The velocity of the product droplet is the same as that of the parent droplet.

The KH–RT model

In the KH–RT model, it is assumed that primary breakup occurs mainly because of the KH instability and that the RT instability causes secondary breakup as shown in Figure 8. The liquid breakup length L is calculated using the equations introduced by Grant and Middleman [9].

$$L = 8.51 d_0 We_f^{0.32}. \quad (7)$$

In region A, the droplet is detached from the liquid column by the KH instability. Once detached the secondary breakup occurs by the RT instability in region B.

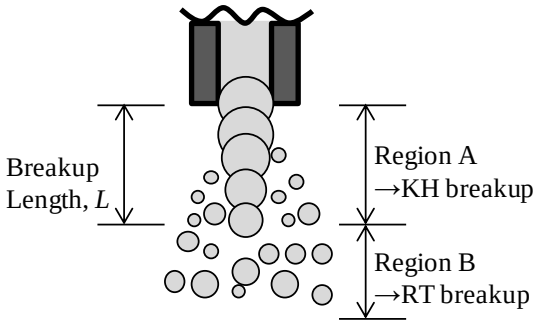

Figure 8 Concept of the KH–RT breakup model

The KH model

According to Reitz [10], the KH breakup is governed by the frequency Ω_{KH} and the

corresponding wavelength Λ_{KH} of the fast growing KH wave.

$$\Lambda_{KH} = \frac{9.02r\left(1+0.45\sqrt{Z}\right)\left(1+0.4T^{0.7}\right)}{\left(1+0.865\,We_g^{1.67}\right)^{0.6}} \tag{8}$$

$$\Omega_{KH} = \frac{0.34+0.38\,We_g^{1.5}}{(1+Z)\left(1+1.4T^{0.6}\right)}\sqrt{\frac{\sigma}{\rho_p r^3}} \tag{9}$$

$$Z = \frac{\sqrt{We_l}}{Re_l} \qquad We_l = \frac{\rho_l U_r^2 r}{\sigma}$$

$$Re = \frac{U_r r}{v_l} \qquad T = Z\sqrt{We_g} \tag{10}$$

$$We_g = \frac{\rho_g U_r^2 r}{\sigma}$$

Here σ, ρ_g, U_r, ρ_l, and v_l are, respectively, the surface tension, gas density, magnitude of the relative velocity between the two phases, liquid density, and liquid viscosity, respectively.

During the breakup, the droplet radius decreases to the critical radius r_{KH} at a uniform rate. In this case, the critical droplet radius r_{KH} and the breakup time τ_{KH} are given by Ref. [10]

$$r_{KH} = B_0\Lambda_{KH}\,, \tag{11}$$

$$\tau_{KH} = \frac{3.726B_1 r}{\Omega_{KH}\Lambda_{KH}}\,, \tag{12}$$

$$\frac{\mathrm{d}r}{\mathrm{d}t} = \frac{r - r_{KH}}{\tau_{KH}}\,, \tag{13}$$

where the model constant $B_0 = 0.61$ and $B_1 = 40$.

The RT model

The equations for the wavelength Λ_{RT} and the frequency Ω_{RT} of the fastest growing wave are given by Ref. [11]

$$\Lambda_{RT} = 2\pi C_{RT}\left(\frac{3\sigma}{-(\vec{g}+\vec{a})(\rho_p-\rho_f)}\right)^{1/2} \tag{14}$$

$$\Omega_{RT} = \left(\frac{2}{3\sqrt{3}\sigma}\frac{\left[-(\vec{g}+\vec{a})(\rho_p-\rho_f)\right]^{3/2}}{\rho_p+\rho_f}\right)^{1/2} \tag{15}$$

where $\vec{g}$ and $\vec{a}$ are the gravity acceleration in the direction of travel and the drag force, respectively. C_{RT} given by Ref. [12] is 0.2. If the waves continue to grow after the breakup time τ_{RT}, the droplet is split into small droplets with the radius r_{RT}. In the RT breakup, τ_{RT} and r_{RT} are defined by Ref. [12]

$$r_{RT} = 0.5\Lambda_{RT} \tag{16}$$

$$\tau_{RT} = \frac{C_\tau}{\Omega_{RT}} \tag{17}$$

where the model constant C_τ is 1.0.

The KH-TAB model

We propose a breakup model that combines the KH and TAB models. The KH model is used for the primary breakup in the area of liquid breakup length L (Figure 8). Beyond the dominant area of the primary breakup, the TAB model is used.

Results and discussion

Comparison of spray structure

The spray structure 6 ms after the injection started is shown in Figure 9. The contour of the numerical results shows the diameter of the droplets. Pulse sprays affecting each other can be observed. All the breakup models show that far away from the nozzle tip, the diameter of the droplets is small. The spray structures in the numerical results are in good agreement with those observed from the experimental results.

Comparison of spray flux and droplet size distribution

The KH–TAB model results for the spray flux and SMD as a function of time are shown in Figure 10 for the first 160 ms after the injection started. In early stage, these values have change because of pulse sprays. The spray flux and SMD have reached a steady-state value which is in agreement with the experimental results.

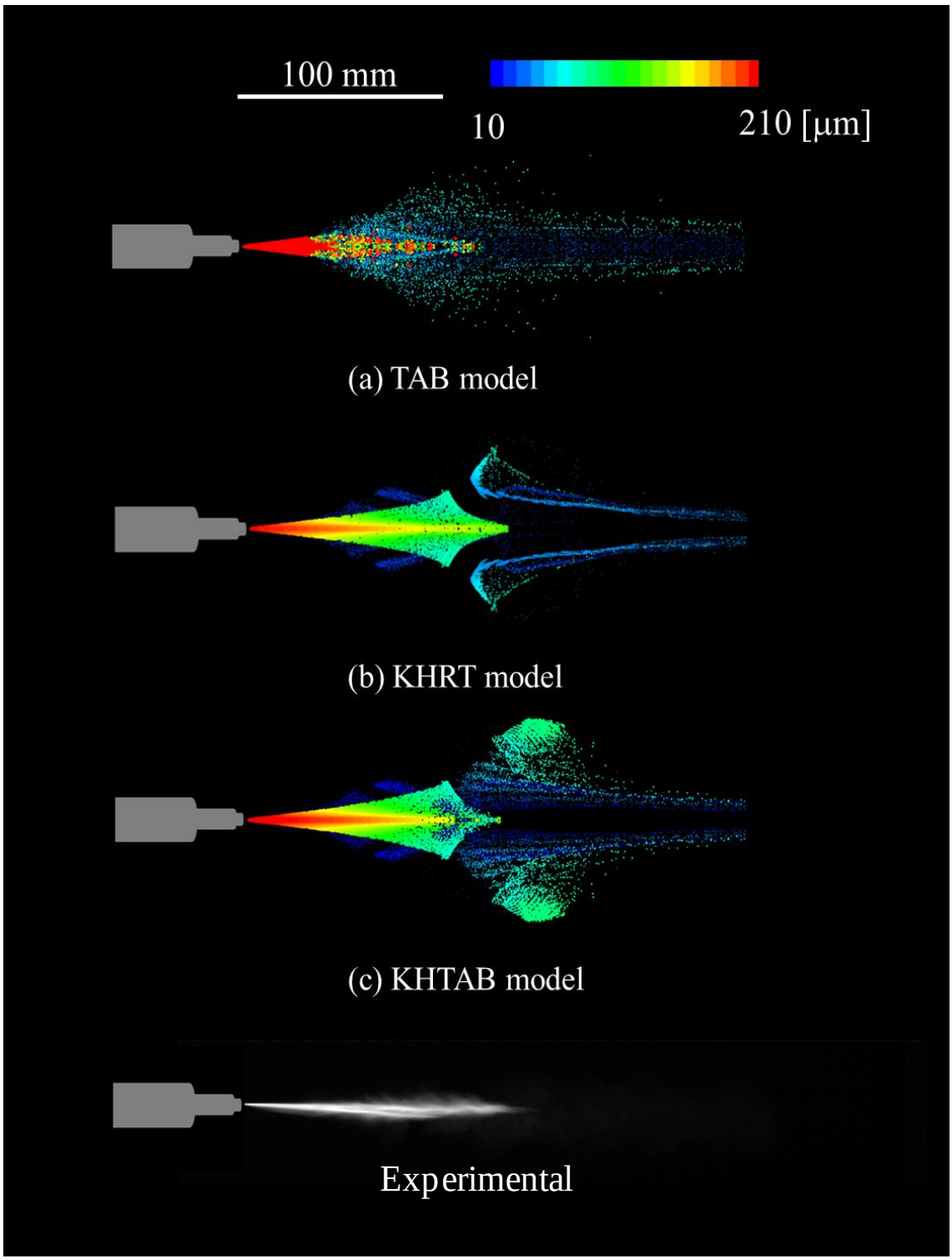

Figure 9 Numerical and experimental results of spray distribution

Spray flux

Figure 11 shows the radial distribution of the spray flux 200 mm downstream from the nozzle tip for the experiment and the three model results. The spray flux of numerical results at 0, 0.005, and 0.01 m is in good agreement with the measurements.

For the KH–RT model, the spray flux at 0.015 m is underestimated in comparison with the experimental results. In terms of this model, it is difficult to express the dispersion of the spray under atmospheric pressure.

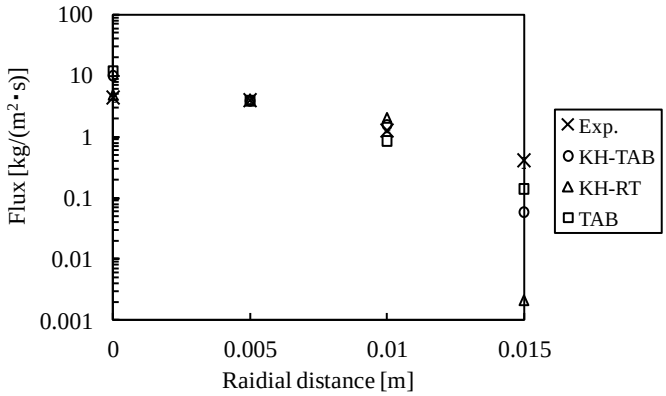

Figure 11 Radial distribution of spray flux at 160 ms after start of injection

Size distributions

Table 6 shows the numerical and experimental results for the SMD 200 mm downstream from the nozzle tip. For the KH–RT and TAB models, SMD is overestimated in comparison with the experimental results. The results produced by the KH–TAB model are in good agreement with those obtained by measurements.

Table 6 Numerical and experimental results for SMD at 160 ms after start of injection

SMD [μm]			
Exp.	KH–TAB	KH–RT	TAB
20.0	21.4	34.2	43.3

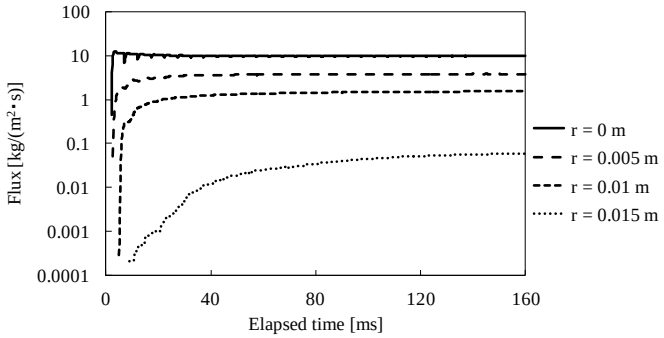

(a) Spray flux

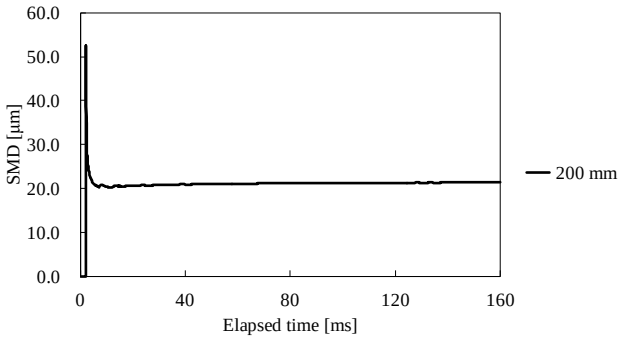

(b) SMD

Figure 10 Spray flux and SMD as a function of time by KH-TAB

Conclusion

In this study, we investigated the optimization of breakup models for high-pressure pulse spray in a stationary combustor. The following results were obtained.

・For the KH–RT model, the spray flux at the outer part of the spray was underestimated in comparison with the experimental results. Thus, this model does not effectively express the dispersion of the spray at this condition. The numerical results using the other models are in good agreement with those obtained by measurements.

・The KH–RT and TAB models overestimated the SMD compared with the experimental results. The numerical results produced by KH–TAB are in good agreement with those obtained by measurements.

Thus, the KH–TAB model shows good agreement with two important measurement results. From our numerical simulation of spray flow under atmospheric pressure for a stationary combustor in a large space, we conclude that the KH–TAB model is the most suitable model.

ACKNOWLEDGEMENTS

This work is supported by KAKENHI（22360318）. I am deeply grateful to KAKENHI.

REFERENCES

[1] Lee C.S., Park S.W., An experimental and numerical study on fuel atomization characteristics, *Fuel*, **81**, 2417-2423 (2002)

[2] Som S., Aggarwal S.K., Effects of primary breakup modeling on spray and combustion characteristics, *Combustion and Flame*, **157**, 1179-1193 (2010)

[3] Kim S., Hwang J.W., Lee C.S., Experiments and modeling on droplet motion and atomization of diesel and bio-diesel fuels in a cross-flowed air stream, *International Journal of Heat and Fluid Flow*, **31**, 667-679 (2010)

[4] Wang X., Huang Z., Kuti O.A., Zhang W., Nishida K., Experimental and analytical study on biodiesel and diesel spray characteristics under ultra-high injection pressure, *International Journal of Heat and Fluid Flow*, **31**, 659-666 (2010)

[5] Yusaku Y., Development of High-Temperature Catalytic Combustor with Starting Burner, *Journal of the Gas Turbine Society of Japan*, **34**, 3, 64-71 (2006)

[6] Crowe C.T, On models for turbulence modulation in fluids-particle flows, *Int. J. Multiphase flow*, **26**, 719-727 (2000)

[7] Roe P. L., Some contributions to the modeling of discontinuous flows, *Lectures in Applied Mathematics*, **22**, Springer-Verlag, Berlin, 163-193(1985)

[8] O'Rourke P.J., Amsden A.A., The TAB Method for Numerical Calculation of Spray Droplet Breakup, *SAE paper*, 872089 (1987)

[9] Grant R.P., Middleman S., "NEWTONIAN JET STABILITY", *AICHE JOURNAL*, **12**, 669-678 (1966)

[10] Reitz R. D., Modeling Atomization Processes in High-Pressure Vaporizing Sprays, *Atomization and Spray Technology*, **3**, 309-337 (1988)

[11] Bellman R., Pennington R.H., Effects of surface tension and viscosity on Taylor instability., Quart Appl Math, **12**, 151-162 (1953)

[12] Beale J.C., Reitz R.D., Modeling Spray Atomization with the Kelvin–Helmholtz /Rayleigh–Taylor Hybrid Model, *Atomization and Sprays*, **9**, 623-650 (1999)